Definition of thermal comfort of crops within naturally ventilated greenhouses

Shahad Al-Rikabi, Enrica Santolini, Beatrice Pulvirenti, Marco Bovo, Alberto Barbaresi, Daniele Torreggiani, Patrizia Tassinari

Department of Agricultural and Food Sciences, University of Bologna, Italy

Abstract

Controlling the microclimate conditions inside a greenhouse is very important to ensure the best indoor conditions for both crop growth and crop production. In this regard, this paper provides the results of a novel approach to study a greenhouse, aiming to define a porous media model simulating the crop presence. At first, an experimental campaign was carried out to evaluate air temperature and air velocity distributions in a naturally ventilated greenhouse with sweet pepper plants cultivated in pots. Then, the main aspects of energy balance, in terms of mass transfer and heat exchange, and both indoor and outdoor climate conditions were combined to set up a computational fluid dynamics model. In the model, in order to simulate the crop presence and its effects, an isotropic porous medium following Darcy's law was defined based on the physical characteristics of the crops. The results show that the porous medium model could accurately simulate the heat and mass transfer between crops, air, and soil. Moreover, the adoption of this model helps to clarify the mechanism of thermal exchanges between crop and indoor microclimate and allows to assess in more realistic ways the microclimate conditions close to the crops.

Correspondence: Marco Bovo, Department of Agricultural and Food Sciences, University of Bologna, viale G. Fanin 48, Bologna, 40127, Italy.
E-mail: marco.bovo@unibo.it

Key words: CFD simulation; energy balance model; porous media; plant canopy; solar radiation.

Conflict of interest: the authors declare no potential conflict of interest.

Received: 3 March 2023.
Accepted: 24 August 2023.

Journal of Agricultural Engineering 2023; LIV:1540
doi:10.4081/jae.2023.1540

Introduction

Crop production through greenhouses has been considered the best approach to increase the growth and development of plants by creating the right microclimate for the crops (Ghoulem *et al.*, 2019). Microclimate parameters inside the greenhouse are very critical to ensure crop growth, and controlling these parameters will result in avoiding problems such as high air temperature which is common during the summer season (Gruda *et al.*, 2019). Therefore, the airflow pattern and thermal behavior of the greenhouse are considered the most important design features in order to keep crop transpiration and photosynthesis at acceptable levels. Natural ventilation is a cost-effective approach of controlling the microclimate parameters inside the greenhouse, it provides the transportation of mass and heat between indoor climate conditions and the external environment while saving energy (Santolini *et al.*, 2018). Adopting the natural ventilation in the greenhouse design can facilitate the control of the microclimate parameters such as air temperature, air humidity and CO_2 concentration (Limtrakarn *et al.*, 2012). Therefore, natural ventilation is considered to be one of the most important production factors because it affects climatic control and crop quality throughout the year (Molina-Aiz *et al.*, 2004). The application of computational fluid dynamics (CFD) technology in the agriculture field has mainly focused on greenhouse microclimate simulation. The use of CFD facilitates the analysis of many aspects as the study scale, the crop type, the weather conditions, and the microclimate parameters (Bournet and Rojano, 2022; Norton *et al.*, 2007). The use of CFD allows the simulation of realistic scenarios through the application of the three conservation equations of the fluid (*i.e.*, mass, momentum, and energy), and combines the fluid turbulence model to simulate and predict the airflow pattern and the spatial distribution of factors such as air temperature and air humidity in the greenhouse (Bartzanas *et al.*, 2013). CFD tools can also provide the possibility to add resource terms through the user-defined function (UDF) to represent the interaction between crops and the surrounding environment (Bekraoui *et al.*, 2022; Versteeg and Malalasekera, 2007). 3D simulations in a multispan greenhouse with active crops have been recently developed, analyzing temperature distribution, crop transpiration model and numerical radiation model (Boulard *et al.*, 2017). Heat transfer in a greenhouse is composed of three contributions: convection, conduction and radiation. Convection is a process of heat transfer through a fluid medium due to the combined effects of buoyancy and thermal expansion. In this process, warmer and less dense air rises while cooler and denser air descends, creating a circulation pattern. This circulation can be driven by a variety of sources such as differences in temperature between solid surfaces of walls, the ground, the crops and the air (Roy *et al.*, 2002). Conduction in a greenhouse is the process by which thermal energy is transferred from one part of the greenhouse structure to another, such as from the air to the soil or from the soil to the air (Maslak, 2015). This process is due to the ther-

mal conductivity, which is the capacity of a material to transfer heat from one region to another (Burger *et al.*, 2016). The distribution of solar radiation in a greenhouse has a significant impact on crop transpiration and photosynthesis. It is highly dependent on greenhouse design, structure materials, covering materials, and weather conditions (Wang and Boulard, 2000; Santolini *et al.*, 2019). More recently, Santolini *et al.* (2022) studied the shading screen effect on the microclimate inside of the greenhouse, studying the possibility of controlling the solar radiation that passes into the greenhouse by three different shading screens, so, to reduce the thermal gain and reach a thermal comfort by coupling solar radiation model with the shading screens mode. The main objective of this study is to focus on the indoor climate distribution in a cultivated greenhouse conditioned with natural ventilation. It also investigates the effects of different solar radiation loads, with the novelty use of a radiation model coupled with local wind directions and profiles on the thermal comfort of the crops within the greenhouse. The study is numerically analyzed through the CFD model conducted by the software Star-CCM+ (Simcenter STAR-CCM+ Academic PowerOn Demand, Siemens 2021). Experimental measurements were used to validate the numerical model. Given this main objective, a series of different scenarios were analyzed for investigating the behavior of crops in response to the thermal distribution due to different solar positions throughout the day in a naturally ventilated greenhouse.

Materials and Methods

Description of the case study

The study has been developed in the greenhouse of the Department of Agricultural and Food Sciences of the University of Bologna, Italy. The greenhouse is located in Imola (44.337340°N latitude, 11.718647°E longitude, and 72m of altitude), the climate in Imola is classified as humid subtropical, with mild winters and hot summers. The town is situated in a basin and is surrounded by hills, which can have a significant impact on the local weather patterns. The greenhouse covers an area of 304.8 m^2 (12.7m long and 24m wide). The greenhouse consists of three spans (each one has a height of 4m at eave, and a maximum height of 5.5m, with a 40% pitch slope) made of steel and covered by 4mm thick glass with a concrete ground (Figure 1).

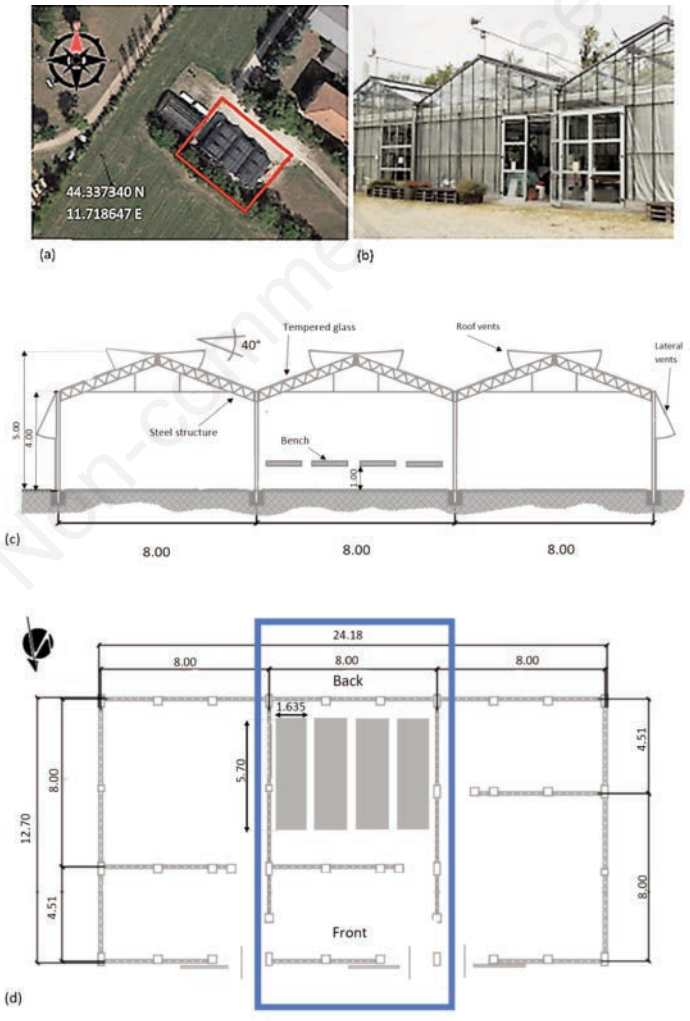

Figure 1. The case study greenhouse. (**a**) Aerial view; (**b**) lateral view; (**c**) vertical transverse section; (**d**) plan view of the layout with the blue rectangle indicating the bay considered in the study.

The study was conducted in the middle span (12.7×8.0m^2) which is separated from the two other spans by a glass wall and has a separate access door. The span is equipped with two continuous roof vents on both sides along the length of the span, with an opening angle of 25°, these vents are crucial to guarantee the natural ventilation inside the greenhouse. The span has 4 polycarbonate benches, one bench was stocked with young sweet pepper (*i.e.*, *Capsicum Annuum L.*), potted in 10 cm high containers. The plants were uniformly placed in 150 pots and distributed in 6 columns on the bench (size of the bench 1.64m wide, 5.7m long, and 1.0m high). The plant density was 16.09 pots/m^2. The average plant height was about 15cm. Plants were watered on the second day of the experiment campaign. The layout of the greenhouse is shown in Figure 1. Each span is independent from others; therefore, the middle span ventilation is not affected by the opening configuration of the lateral spans.

Description of the numerical model

The computational fluid dynamics approach is suitable for developing models that explain the relationship between climate variables and the behavior of airflow inside the greenhouses by using the Navier-Stokes conservation equations for the mass, momentum, and energy (Kinyua, 2017; De la Torre-Gea *et al.*, 2011). The CFD simulations are carried out by Simcenter STAR-CCM+ software (Simcenter STAR-CCM+ Academic PowerOn Demand, Siemens 2021). CFD tool allows simulating complex phenomena, especially for the assessment of the indoor microclimate starting from the knowledge of the outdoor environmental parameters. In the CFD simulations, the calculation domain is divided into elementary volumes, defined as cells to solve the conservation equations to predict variables such as fluids pressure, velocity, and temperature. These variables are obtained in each control volume through an iterative procedure that continues until the nonlinear system of equations has a converged solution. The calculation domain in the case at hand, has an area of 25661 m^{2}and is 27 m high. The domain includes the greenhouse, the floor, the benches, the pots, and the plants. The geometrical domain was defined as an octagon to accurately symbolize the directions of airflow, the left side of the calculation domain represents the East, East-South, and South side. The domain adopted in the simulations is shown in Figure 2.

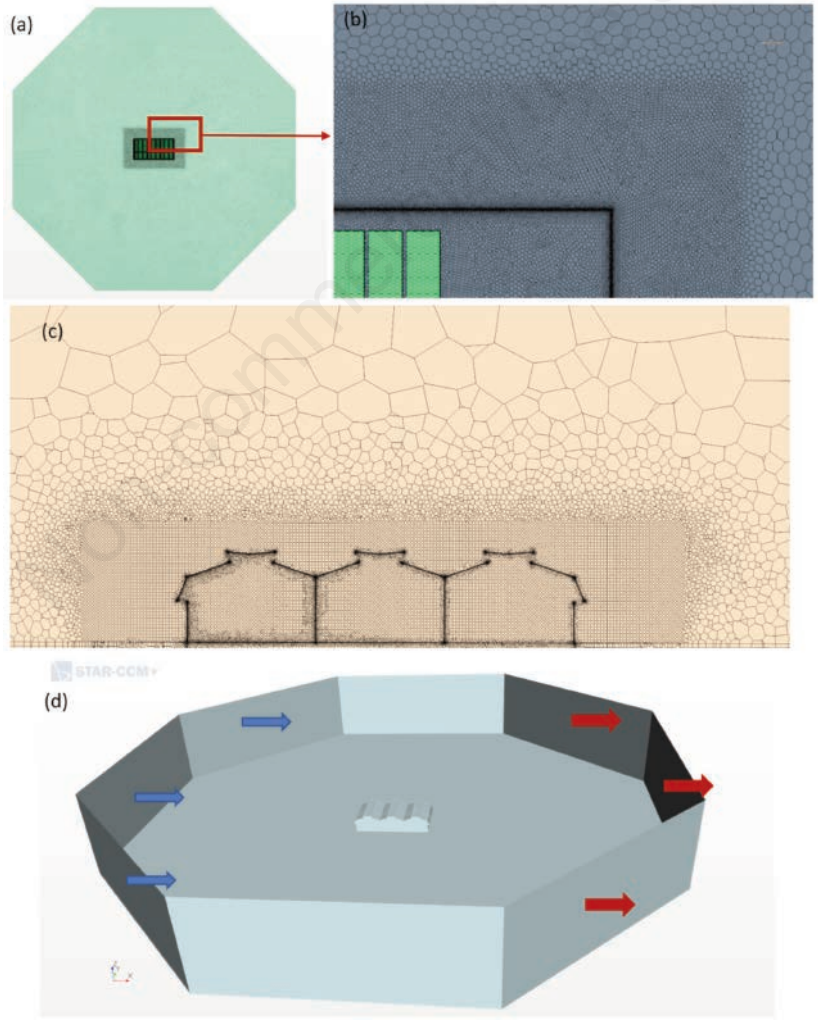

Figure 2. Numerical model used in the work. (**a**) Top view of the entire domain; (**b**) detail of the mesh close to a corner of the greenhouse; (**c**) view of a vertical section of the mesh; (**d**) geometrical computational domain including the greenhouse, inlets (South, South-East, East) indicated by the blue arrays and outlets (East, East-South, and South) indicated by the red arrays.

A polyhedral mesh was chosen to limit the numerical diffusion of errors and facilitate calculation convergence. In STAR-CCM+, a specific dualization scheme is used to automatically transform an underlying tetrahedral mesh into a polyhedral mesh. The polyhedral meshing model generates random polyhedral-shaped cells that are relatively faster and more efficient to build than a tetrahedral mesh for a given surface. The mesh was refined around the crops, benches and in areas where strong gradients may occur, *e.g.*, close to the ground and the walls (Figure 2).

Fundamental equations

The flow in the greenhouse is considered to be steady state, incompressible, and turbulent. The Navier-Stokes transport equation, representing the distribution of the mass, velocity components, and temperature in the domain, is reported in Eq.(1):

$$\frac{\partial \phi}{\partial t} + \frac{\partial}{\partial x_j}(u_j \phi) = \frac{\partial}{\partial x_j}(\Gamma_\phi \frac{\partial \phi}{\partial x_j}) + S_\phi \quad (1)$$

where: u_j represents components of fluid velocity, Γ is the diffusion coefficient, and S_ϕ is the source term.

The standard k-ε turbulence model within the domain has been adopted (Launder and Spalding, 1974). This model introduced the equations of kinetic energy k and the dissipation rate ε:

$$k = \frac{u_*^2}{\sqrt{C_\mu}}\left(1 - \frac{z}{\delta}\right) \quad (2)$$

$$\varepsilon = \frac{u_*^2}{kz}\left(1 - \frac{z}{\delta}\right) \quad (3)$$

where: δ is the atmospheric boundary layer depth and C_μ is a coefficient used to define the eddy viscosity in k-ε models. A standard value of C_μ=0.09 has been assumed. The equations were numerically solved according to the finite volume method implemented in the software STAR-CCM+. The convergence criteria for the continuity, momentum and energy was 10^{-6} and it was reached after 3000 iterations. The boundary conditions derived from measurements are reported in Table 1. They were used to introduce the effect of outdoor parameters including air temperature, wind velocity, and air humidity. At the entrance (the inlets) of the calculation domain in Figure 2 on the left side (*i.e.*, South, South-East, East) a uniform temperature obtained from the weather station data was applied, whereas the horizontal velocity profile was derived from the experimental data by using the log-law fit:

$$U(z) = \frac{u_*}{K} ln\left(\frac{z + z_0}{z_0}\right) \quad (4)$$

where: U(z) is the horizontal velocity (m s^{-1}), u* is the friction wind velocity, K is the von Karman's constant, z is the height above the ground and z_0 is surface roughness.

As said, uniform air temperature and air humidity conditions, obtained from the measurements, were applied at the inlet. Then, a no-slip boundary wall condition was applied to all the wall elements in the domain including greenhouse walls, benches and ground. This condition assumes that the velocity of air particles at the boundary wall is zero, meaning that the fluid particles do not move relative to the wall elements. A convective boundary condition was applied to the soil inside the greenhouse adopting a heat transfer coefficient of 13 $Wm^{-2}K^{-1}$ calculated using the formula for steady-state convection heat transfer. The soil outside the greenhouse was assumed to be adiabatic, since the focus of the study was the evaluation of the microclimate inside the greenhouse. In order to ensure a parallel flow, a symmetry boundary condition has been imposed on the top side (*i.e.*, sky) and the lateral sides of the calculation domain (*i.e.*, North-East and South-West). Radiation was simulated directly using the solar load feature built-in STAR-CCM+, and was defined on all the regions, taking into account the geographical position of the greenhouse. In order to take account of the overhead heating, heat flux was applied along the greenhouse walls and along the ground surface. STAR-CCM+ automatically conducted the coupling between radiative and convective transfer for the solid and fluid interfaces, and the porous media was considered as a semi-transparent media interfacing with radiation. The software provided the radiative balance for each mesh of the porous media. The energy balance equation, which calculates the sensible and latent heat exchanges between each cell of the porous media and the air, used this global net radiative flux as its source term (Fatnassi *et al.*, 2017).

At the exit of the calculation domain (*i.e.*, North, North-West, West), a pressure outlet condition (*i.e.*, atmospheric pressure) was imposed. Table 1 reports the values of the experimental measurements used as initial boundaries and boundary conditions in the simulations.

Radiative submodel

A radiative submodel was introduced in order to take account of the thermal contribution of radiative transfers between the surfaces in the greenhouse. The Surface to Surface (S2S) model was chosen because of its ability to simulate the radiation generated by the sun by using the Solar Calculator feature implemented STAR-CCM+. The solar calculator is able to compute the direct and diffuse solar radiation depending on the geographical location of the greenhouse and the time of carrying out the experiments (Saberian and Sajadiye, 2019). The values of direct solar flux and diffuse solar flux obtained according to the greenhouse coordinates (*i.e.*, 44.337340° Latitude; 11.718647° Longitude) on April, 29th at 13:00, are 670Wm^{-2} and 220Wm^{-2}, respectively. The gray spectrum model considers the full length of the thermal spectrum as a simplified method to represent the environment around the continua. Finally, the thermal properties of the greenhouse materials used in the model are reported in Table 2 and Table 3.

Table 1. Initial parameters and boundary conditions.

Parameter	Value
External air temperature (°C)	19.6
Inside air temperature (°C)	23.4
Concrete temperature (°C)	22.8
Cultivation bench temperature (°C)	28.0
Glass wall temperature (°C)	29.8
Inlet velocity at a level of 5 m (ms^{-1})	1.75
Convection heat transfer coefficient of greenhouse ($Wm^{-2}K^{-1}$)	25.0
Greenhouse thermal resistance (m^2KW^{-1})	0.2

Crop model

The effect of the crops within the greenhouse has been modeled as a momentum sink, related to the drag force on the leaves. The crops have been modeled as a homogeneous porous medium which creates a pressure drop based on Darcy-Forchheimer law (Boulard and Wang, 2002). This pressure drop is considered a negative source term in the momentum equations. The sink of momentum due to the drag effect by a crop unit volume can be evaluated by means of the following well-known equation (Thom, 1971):

$$S = -\rho_a \ LAD \ C_D \ V^2 \quad (5)$$

where: LAD is the leaf area density ($m^2\ m^{-3}$), V is the air velocity, ρ_a is the air density (kg m^{-3}), and C_D is the dimensionless drag coefficient. With reference to the work of Molina-Aiz *et al.* (2006), a sweet pepper crop cultivated in a greenhouse, has a value of drag coefficient equal to C_D =0.31 and LAD =6 m^2m^{-3}.

Energy balance model

The porous medium representing the crops was divided into elementary volumes to model heat transfer between the crops and the indoor environment. Since sweet pepper crops are cultivated in pots on benches, conductive transfers between the benches and the crops can be neglected (Kichah *et al.*, 2012). The energy balance depends on environmental factors and the most important are solar radiation, air humidity, air temperature, and air velocity. In the study, since the software STAR-CCM+ does not have an integrated model to simulate the energy balance, a UDF was built to compute heat and resistances, for each cell in the crop boundary zone.

Table 2. Thermal characteristics of the materials used as initial conditions.

Material	Density (ρ) (kg m^{-3})	Thermal conductivity (κ) (W m^{-1} K^{-1})	Specific heat (C_p) (J kg^{-1} K^{-1})
Glass	2530.0	1.2	840.0
Poly-carbonate	1200.0	0.2	1170.0
Soil	1620.0	1.3	1480.0
Concrete	2200.0	1.5	1000.0

Table 3. Radiative characteristics of the materials used as initial conditions.

Material	Absorbance (-)	Emissivity (W m^{-2})
Glass	0.7	0.90
Poly-carbonate	0.1	0.90
Soil	0.9	0.93
Concrete	0.6	0.88

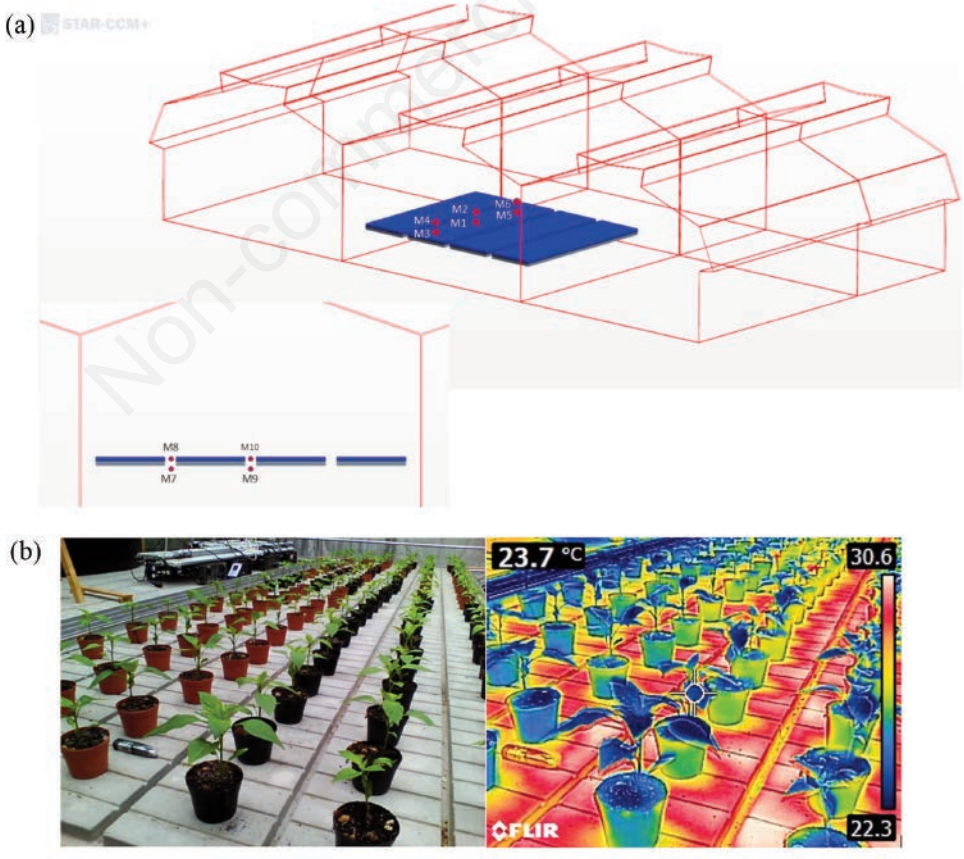

Figure 3. Experimental measurements. (**a**) Measurement points highlighted by red points; (**b**) temperature measurements with thermal camera.

A radiative flux reaches each elementary volume and converts it into latent heat flux and sensible heat flux following the equation:

$$G_a = Q_s + Q_l \quad (6)$$

where: G_a (Wm^{-3}) is the radiative flux absorbed by each cell in the porous media, Q_s (Wm^{-3}) is the sensible heat flux at the canopy level and represents the heat flux transferred between the crops (*i.e.*, porous media) and the air in the greenhouse, and Q_l (Wm^{-3}) is the latent heat flux that represents the transpiration process. The sensible heat flux Q_s produced by the crops can be calculated as (Fatnassi *et al.*, 2017):

$$Q_s = LAD\ \rho_a\ C_p\ (T_l - T_a)/r_a \quad (7)$$

where: r_a is the leaf aerodynamic resistance, assumed equal to r_a=271 sm^{-1} following (Baille *et al.*, 1994), ρ_a is the air density (kg m^{-3}), C_p is the air specific heat at constant pressure (J $kg^{-1}\ k^{-1}$), T_a is the air temperature, and T_l is the leaf temperature. Following Bouhoun Ali *et al.* (2018), the latent heat flux can be expressed as:

$$Q_l = \lambda\ LAD\ \rho_a\ \frac{(\omega_L - \omega_a)}{(r_a - R_s)} \quad (8)$$

where: λ is the latent heat of vaporization of water, set equal to 2500 kJ kg^{-1} following Bouhoun Ali *et al.* (2014), w_L and w_a are the absolute humidity of leaf and air (kg kg^{-1}), and R_s is the leaves stomatal resistance (sm^{-1}). The latter plays a crucial role in the transpiration flux, and can be defined as a function of global radiation and vapor pressure deficit, following (Zhang and Kacira, 2022) it can be expressed as:

$$R_s = 200\ \frac{(31+G_a)[1+0.016(T_a-16.49)^2]}{6.7+G_a} \quad (9)$$

Experimental set-up

Measurements were collected for three days (*i.e.*, 28th, 29th and 30th) in April 2021. Inside the greenhouse, a set of sensors were placed to provide inputs and data, to validate the CFD model, and to check the interaction between the crop growth and the indoor conditions. Two hot wire anemometers Delta Ohm, with uncertainty of 0.01ms^{-1} were used to measure the wind velocity and temperature on different heights and positions. The measurement points M1, M3 and M5 were taken at 10cm above crop level. M2, M4 and M6 were taken at 20cm above the crop level, as shown in Figure 3a. The anemometers were also used to measure the velocity and temperature around the perimeter sides of the bench at 90cm and 1.10 cm above the ground as represented in the M7, M8, M9 and M10 positions shown in Figure 3a.

Indoor air temperature, T_a, and air relative humidity were measured by using five probes (*i.e.*, dataloggers) located on the surface of the benches, and above the benches. The leaf temperature, T_l, and the ground temperature were recorded by using a thermal camera (AVIO) as well as the temperature of the walls (Figure 3b). All the above-mentioned parameters were measured every 5s and averaged over a 10 min period. The measurements for this study were acquired during the three days between 10:00 am and 4:00 pm. The outdoor wind speed, wind direction, air temperature, solar radiation and air relative humidity data were taken from a weather station located on the roof of the greenhouse.

Results and Discussion

A first set of simulations has been done to validate the model and by comparing numerical results with experimental outcomes. Then, the thermal comfort of crops has been investigated for six different meteorological configurations.

Validation of the numerical model

The experimental data used for the validation of the numerical model have been taken from the second day of the campaign, the 29th of April, 2021 at 13:00 when the weather was more stable with partial clouds.

The numerical air temperatures and air velocities of the ten measurement points have been compared with the corresponding points in the experimental test. It is observed from Figure 4 that the results of the simulation are in good agreement with the experimental data. The highest difference in temperature was 1.5°C at point M6. Similarly, the maximum difference in terms of velocity was 0.04 ms^{-1} also at point M6. With reference to the results of the numerical simulation, the horizontal distribution of the temperature on the crops was heterogeneous and with a difference in temperature up to 3°C, due to the combined influence of radiation and

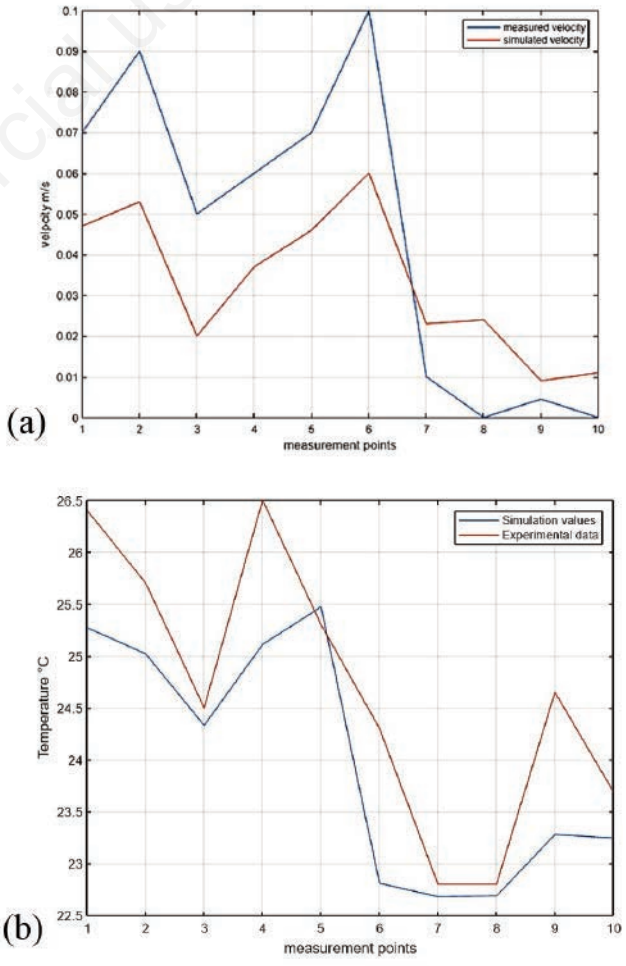

Figure 4. Comparison between measured and simulated (**a**) air velocity and (**b**) air temperature.

convective heat transfer, as shown in Figure 5a. Moreover, the vertical distribution of crop temperature is hardly noticeable due to the low height of the porous media. The wind velocity has a non-uniform distribution inside the greenhouse, combined with a vortex in the middle of the span, with other two small vortices close to the walls of the span (Figure 5b). The airflow above the crops has a velocity range of around 0.2ms^{-1}, while the airflow passing through the porous media has a lower velocity due to the presence of the crops. The reliability of the numerical model was evaluated using the Root Mean Square Error (RMSE), which demonstrated the good agreement between simulated and measured data, the RMSE of the temperature and air velocity were 1.01°C and 0.05 ms^{-1}. These RMSE values show alignment with the values reported in previous studies, with Bouhoun Ali *et al.* (2018) that obtained RMSE values of 0.49°C for temperature and 0.05 ms^{-1} for air velocity, and Teitel *et al.* (2022) reported a RMSE range of 0.86-1.57°C for the temperature. The analysis of the overall results demonstrates a good agreement between the simulation and the experimental test. The CFD model seems capable of performing realistic evaluations of the microclimate inside the greenhouse also with relation to the thermal contribution of the solar radiation. The porous medium model can reliably simulate heat and mass transfer between the crops and the surrounding environment.

Numerical applications

Once the model has been validated, it could reliably be used to predict solar radiation distribution with different sun positions at different seasons. Since the values of direct and diffuse solar irradiation change with the sun altitude (PVGIS, 2023), analysis of different solar positions throughout the day has been carried out on four cultivated benches in the middle span of the greenhouse. Six different scenarios have been selected to represent these variations along with changing in air temperature and wind speed.

The six configurations have been divided into two groups: i) the first group has a velocity profile of 1.75 ms^{-1} at the inlet with three different settings of sun position, *i.e.*, at noon where the sun is vertical to the greenhouse with 63° elevation with reference to the horizon, when the sun is diagonal to the greenhouse with 15° elevation, and at midnight when there is no impact of the sun; ii) the second group has a velocity profile of 4ms^{-1} at the inlet, to investigate the effect of wind velocity on the temperature distribution inside the greenhouse, with the same configurations of sun positions considered for the first group.

Analysis of air temperature distribution

In general, the temperature pattern in the six cases reveals that the greenhouse microclimate is warmer than the outdoor environment and the roof vents work as inlet for the cold air coming from outside and as outlet for inside warm air. The temperature distribution in the vertical cross-section in the middle span of the greenhouse (Figure 6), demonstrates the higher heat transfer values on the glass walls, soil, and ground, which are related to higher surface heat transfer coefficient on these regions. The observed temperature in the first group (*i.e.*, cases 1, 2, and 3) with a wind velocity profile of 1.75m*s*$^{-1}$ is higher if compared to the second group (*i.e.*, cases 4, 5, and 6) with 4m*s*$^{-1}$, as shown in Figure 6.

The significant difference in temperature is noticed in case 1 and case 4, the highest increase is, in case 1, of about 5°C with reference to the external conditions, due to the high thermal load and the low wind velocity (Figure 6). In cases 2 and 5, the temperature has a moderate distribution due to less thermal load on the greenhouse. The temperature between the crops and the surrounding air is in the same range. It is noticeable that the soil on the benches in

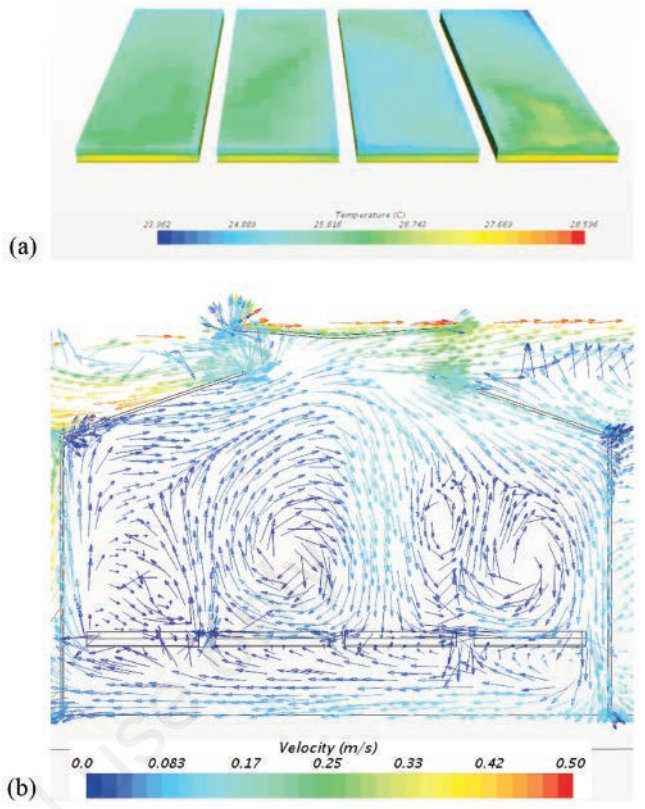

Figure 5. View of (**a**) temperature distribution of the porous media and (**b**) vertical section at the middle of the benches showing the vector distribution of the velocity.

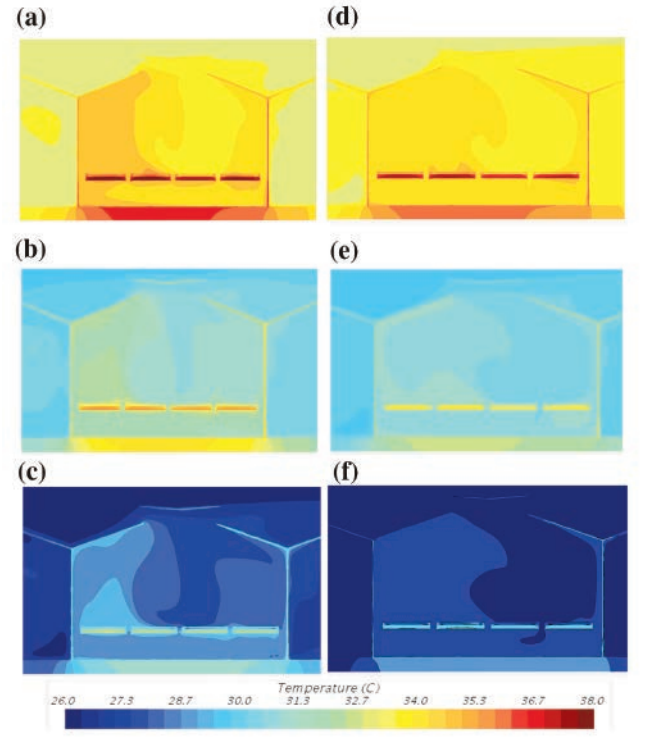

Figure 6. Vertical view of the temperature distribution at middle span: (**a**) case 1, (**b**) case 2, (**c**) case 3, (**d**) case 4, (**e**) case 5, (**f**) case 6.

case 2 is warmer than in case 5 due to lower wind velocity. In cases 3 and 6, when the effect of solar radiation is absent, the overall temperature of the greenhouse is decreasing mainly because of radiative losses. The temperature inside the crops is warmer than the air around it. In case 3, the difference in temperature between the crops and the surrounding air is 2°C, while in case 6, the difference is about 1°C, due to the higher wind velocity (Table 4).

Airflow pattern

Velocity was calculated for each case through a vertical line in the middle of the span. The measurement line starts from the ground, passes through the porous media volume, and reaches the roof. Analysis of the results according to their height and comparing the data with the flow patterns indicates that the roof vents work as inlet and outlet to the span. The wind flow is facing the drag force of the porous media, in addition to the presence of benches which strongly decrease the wind velocity (Figure 7) illustrating the average wind velocity according to the height inside the Case 6 has the highest wind velocity near the roof vents and it takes a similar pattern as case 4 and case 5. The velocity decreases directly with the height of the greenhouse except in two areas, at the level of 2.5m where the air current is being fed by the vortex and close to the ground as the air current is being fed by direct airflow coming from the windward wall and goes beneath the benches. Case 2 and case 3 have no numerically considerable difference according to their average wind velocity. For case 1, case 2, and case 3, which have a wind profile of 1.75 ms^{-1}, the results indicate that the wind distribution around the crops could hardly reach the crops minimum range for the optimum growth (*i.e.*, 0.2-0.7 ms^{-1}). For cases 4, 5, and 6, with a wind profile of 4 ms^{-1}. The overall results closely align with previous findings, (Zhang and Kacira, 2022) reported a velocity range of 0.2-0.5 ms^{-1}, and Roy and Boulard (2005) obtained a velocity range of 0.2-1.5 ms^{-1}. The results indicate that the wind distribution fits the requirements for the crops optimum growth.

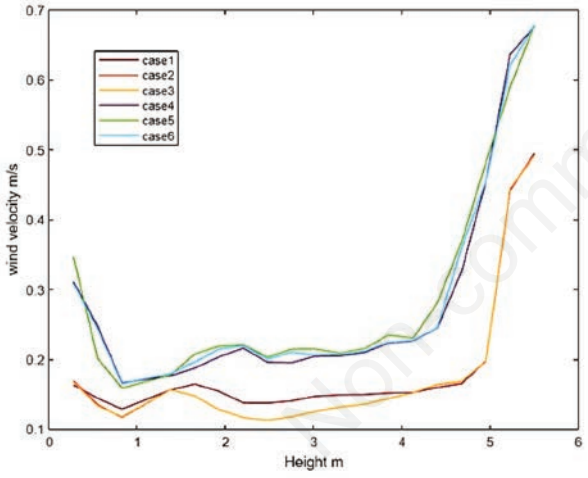

Figure 7. Average wind velocity for the six cases in the middle span, at 9 m from the north side (front) and 11 m from the east side of the greenhouse.

Characterization of crops thermal comfort

In the cases with high contribution of heating due to solar radiation (cases 1 and 4), the airflow enters the greenhouse through the roof vents, leading to a lowering of the temperature at the crop level of about 2°C (see Figure 8 illustrating the temperature distribution at the crop level). Case 4 corresponds to a higher air veloc-

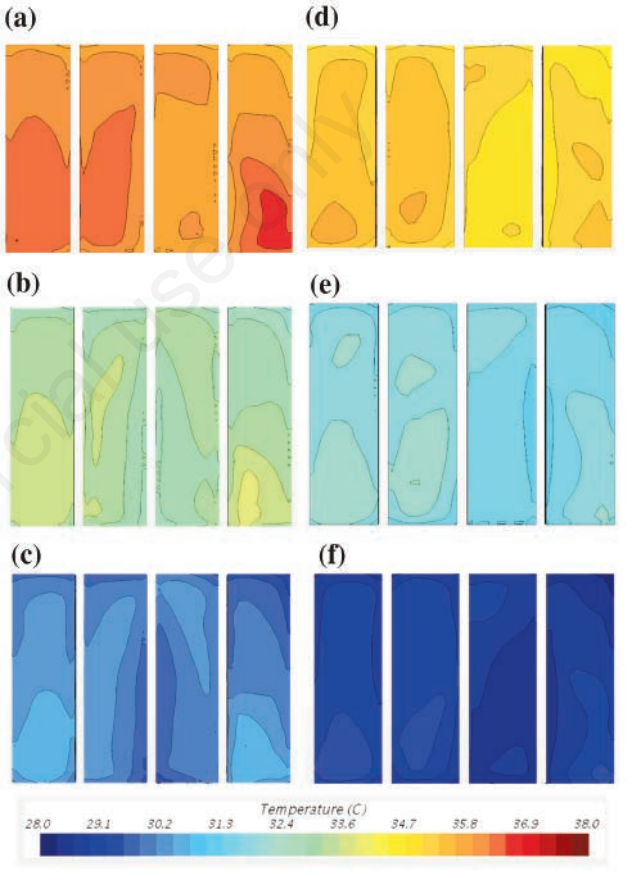

Figure 8. Top view of benches showing temperature distribution at the crop level. (**a**) Case 1; (**b**) case 2; (**c**) case 3; (**d**) case 4; (**e**) case 5; (**f**) case 6.

Table 4. Summary of the six cases numerically investigated in the paper.

Case number #	Simulated time (hh:mm)	Sun position to greenhouse	Outside temperature (°C)	Inlet velocity (ms^{-1})	Direct solar flux (Wm^{-2})	Diffuse solar flux (Wm^{-2})
1	12:00	vertical	33.0	1.75	947.0	237.0
2	19:00	diagonal	29.0	1.75	103.0	26.0
3	00:00	no sun	26.0	1.75	0.0	0.0
4	12:00	vertical	33.0	4.0	947.0	237.0
5	19:00	diagonal	29.0	4.0	103.0	26.0
6	00:00	no sun	26.0	4.0	0.0	0.0

ity around the crops indicating a max reduction in temperature of about 4°C and a better distribution in temperature at a crop level.

In conditions of low contribution of solar radiation (*i.e.*, cases 2 and 5) or conditions with no solar radiation (*i.e.*, cases 4 and 6), a smaller influence of air velocity near the crops was observed. This means that in these cases the thermal comfort of the crops is achieved with smaller values of the air velocity within the greenhouse. The temperature of the crops and the velocity distribution around the crops are two parameters that can be combined in order to achieve the best thermal control of crops within greenhouses. Also, air humidity is an important parameter to monitor, but in naturally ventilated greenhouses the main approach for thermal control is by changing the opening configuration of the vents. Through the analysis of the six different cases, it is possible to understand the influence of higher and lower values of wind velocity and solar radiation on the thermal distribution inside the greenhouse. These results can be used to identify a digital twin of the greenhouse that can be used for improving the management of the greenhouse and also for a better dynamical control of the thermal conditions of crops within the existing one.

Conclusions

CFD simulations, adopting novel modeling elements such as the S2S radiation model coupled with thermal and plant models, were used to numerically investigate the effects of different solar radiation loads, local wind directions and profiles, and indoor climate on a cultivated greenhouse naturally ventilated. An experimental measurement setup was used to validate the numerical model. The CFD model was proven to be an effective method for simulating the crops as a porous media that is able to represent heat transfer between the plants and the surrounding environment, and forecasting solar heat load and temperature distribution inside the greenhouse. The results seem to indicate that by increasing wind velocity, the temperature distribution becomes more homogeneous inside the investigated span of the greenhouse, the porous media temperature decreases by approximately 3°C if compared to the cases with lower velocity. The CFD also investigated the influence of the crops on the indoor climate, as the porous media works as obstacles to the wind flow leading to form several vortices with lower velocities. The results exemplify the appropriate microclimate conditions to reach the thermal comfort of the crops in an energy-efficient greenhouse by depending on natural ventilation and solar radiation. The analysis of temperature and air velocity around the crops in six different test cases highlights that only for particular conditions the indoor thermal range meet the crop best thermal conditions.

References

Baille M., Baille A., Laury J.C. 1994. Canopy surface resistances to water vapour transfer for nine greenhouse pot plant crops. Scientia Horticulturae 57:143-55.

Bartzanas T., Kacira M., Zhu H., Karmakar S., Tamimi E., Katsoulas N., Lee I.B., Kittas C. 2013. Computational fluid dynamics applications to improve crop production systems. Comput. Electron. Agric. 93:303-13.

Bekraoui A., Chakir S., Fatnassi H., Mouqallid M., Majdoubi H. 2022. Climate behaviour and plant heat activity of a citrus tunnel greenhouse: A computational fluid dynamic study. AgriEngineering 4:1095-115.

Bouhoun Ali H., Bournet P.E., Cannavo P., Chantoiseau E. 2018. Development of a cfd crop submodel for simulating microclimate and transpiration of ornamental plants grown in a greenhouse under water restriction. Comput. Electron. Agric. 149:26-40.

Bouhoun Ali H., Bournet P.E., Danjou V., Morille B., Migeon C. 2014. CFD simulations of the night time condensation inside a closed glasshouse: Sensitivity analysis to outside external conditions, heating and glass properties. Biosyst. Eng. 127:159-75.

Boulard T., Roy J.C., Pouillard J.B., Fatnassi H., Grisey A. 2017. Modelling of micrometeorology, canopy transpiration and photosynthesis in a closed greenhouse using computational fluid dynamics. Biosyst. Eng. 158:110-33.

Boulard T., Wang S. 2002. Experimental and numerical studies on the heterogeneity of crop transpiration in a plastic tunnel. Comput. Electron. Agric. 34:173-90.

Bournet P.E., Rojano F. 2022. Advances of computational fluid dynamics (cfd) applications in agricultural building modelling: Research, applications and challenges. Comput. Electron. Agric. 201:107277.

Burger N., Laachachi A., Ferriol M., Lutz M., Toniazzo V., Ruch D. 2016. Review of thermal conductivity in composites: Mechanisms, parameters and theory. Prog. Polym. Sci. 61.

Fatnassi H., Boulard T., Roy J.C., Suay R., Poncet C. 2017. CFD coupled modeling of distributed plant activity and climate in greenhouse. Acta Hortic. 1182:57-64.

Ghoulem M., El Moueddeb K., Nehdi E., Boukhanouf R., Kaiser Calautit J. 2019. Greenhouse design and cooling technologies for sustainable food cultivation in hot climates. Biosyst. Eng. 183:121-50.

Gruda N., Bisbis M., Tanny J. 2019. Impacts of protected vegetable cultivation on climate change and adaptation strategies for cleaner production–A review. J. Clean. Prod. 225:324-39.

Kichah A., Bournet P.E., Migeon C., Boulard T. 2012. Measurement and CFD simulation of microclimate characteristics and transpiration of an Impatiens pot plant crop in a greenhouse. Biosyst. Eng. 112:22-34.

Kinyua D. 2017. A cfd analysis of heat and mass transfer in greenhouses: An introduction. Math. Model. Appl. 2:17.

Launder B.E., Spalding D.B. 1974. The numerical computational of Turbulent flows. Comput. Methods Appl. Mech. Eng. 3:269-89.

Limtrakarn W., Boonmongkol P., Chompupoung A., Rungprateepthaworn K., Kruenate J., Dechaumphai P. 2012. Computational fluid dynamics modeling to improve natural flow rate and sweet pepper productivity in greenhouse. Adv. Mech. Eng. 4:158563.

Maslak K. 2015. Thermal energy use in greenhouses the influence of climatic conditions and dehumidification. Environ. Sci. Agric. Food Sci. Available from: https://www.semanticscholar.org/paper/Thermal-Energy-Use-in-Greenhouses-The-Influence-of-Maslak/f90023ef54a1e48faa708612ff858c846f6f4e50

Molina-Aiz F., Domingo F., Valera D.L., Álvarez A.J. 2004. Measurement and simulation of climate inside Almerıa-type greenhouses using computational fluid dynamics. Agric. For. Meteorol. 125:33-51.

Molina-Aiz F., Valera D., Alvarez A., Madueño A. 2006. A wind tunnel study of airflow through horticultural crops: determination of the drag coefficient. Biosyst. Eng. 93:447-57.

Norton T., Sun D.W., Grant J., Fallon R., Dodd V. 2007.

Applications of computational fluid dynamics (cfd) in the modelling and design of ventilation systems in the agricultural industry: A review. Bioresour. Technol. 98:2386-414.

PVGIS. 2023. Available from: http://re.jrc.ec.europa.eu/pvgis/apps3/pvest.php, accessedonJanuary10th,2013

Roy J.C., Boulard T. 2005. Cfd prediction of the natural ventilation in a tunnel-type greenhouse: Influence of wind direction and sensibility to turbulence models. Acta Hortic. 691:457-64.

Roy, J.C., Boulard, T., Kittas C., Wang S. 2002. PA-Precision Agriculture: Convective and Ventilation Transfers in Greenhouses, part 1: the greenhouse considered as a perfectly stirred tank. Biosyst. Eng. 83:1-20.

Saberian A., Sajadiye S.M. 2019. The effect of dynamic solar heat load on the greenhouse microclimate using CFD simulation. Renew. Energy 138:722-37.

Santolini E., Pulvirenti B., Benni S., Barbaresi L., Torreggiani D., Tassinari P. 2018. Numerical study of wind-driven natural ventilation in a greenhouse with screens. Comput. Electron. Agric. 149:41-53.

Santolini E., Pulvirenti B., Guidorzi P., Bovo M., Torreggiani D., Tassinari P. 2022. Analysis of the effects of shading screens on the microclimate of greenhouses and glass facade buildings. Build. Environ. 211:108691.

Santolini E., Pulvirenti B., Torreggiani D., Tassinari P. 2019. Novel methodologies for the characterization of airflow properties of shading screens by means of wind-tunnel experiments and cfd numerical modeling. Comput. Electron. Agric. 163.

Simcenter STAR-CCM+ Academic Power On Demand, Siemens 2021.

Teitel M., Ozer S., Mendelovich V. 2022. Airflow temperature and humidity patterns in a screenhouse with a flat insect-proof screen roof and impermeable sloping walls – computational fluid dynamics (cfd) results. Biosyst. Eng. 214:165-76.

Thom A.S. 1971. Momentum absorption by vegetation. Q. J. R. Meteorol. Soc. 97:414-28.

De la Torre-Gea G., Soto-Zarazúa D., Lopez-Cruz I., Pacheco I., Rico-García E. 2011. Computational fluid dynamics in greenhouses: A review. Afr. J. Biotechnol. 10:17651-62.

Versteeg H.K., Malalasekera W. 2007. An introduction to computational fluid dynamics: The finite volume method. Pearson Education.

Wang S., Boulard T. 2000. Measurement and prediction of solar radiation distribution in full-scale greenhouse tunnels. Agronomie 20:41-50.

Zhang Y., Kacira M. 2022. Analysis of climate uniformity in indoor plant factory system with computational fluid dynamics (CFD). Biosyst. Eng. 220:73-86.